Journal of Macromolecular Science, Part A
Publication details, including instructions for authors and subscription information:
http://www.informaworld.com/smpp/title~content=t713597274

Molecular Modeling of Interchain Nonbonding Interactions in Blends of Polyacrylonitrile with Poly(Ethylene-*alt*-Maleic Anhydride)

Simona Percec[a]; Joni Gray[a]
[a] BP Chemicals Inc, Cleveland, Ohio

To cite this Article Percec, Simona and Gray, Joni(1995) 'Molecular Modeling of Interchain Nonbonding Interactions in Blends of Polyacrylonitrile with Poly(Ethylene-*alt*-Maleic Anhydride)', Journal of Macromolecular Science, Part A, 32: 8, 1563 — 1575
To link to this Article: DOI: 10.1080/10601329508013697
URL: http://dx.doi.org/10.1080/10601329508013697

J.M.S.—PURE APPL. CHEM., A32(8&9), pp. 1563–1575 (1995)

MOLECULAR MODELING OF INTERCHAIN NONBONDING INTERACTIONS IN BLENDS OF POLYACRYLONITRILE WITH POLY(ETHYLENE-*alt*-MALEIC ANHYDRIDE)

SIMONA PERCEC* and JONI GRAY

BP Chemicals Inc.
4440 Warrensville Center Road, Cleveland, Ohio 44128

ABSTRACT

Molecular modeling has been employed to describe possible spatial arrangements in a miscible blend derived from two polymeric chains involved in weak nonbonding interchain interactions. The two polymers under investigation are polyacrylonitrile (A) and poly(ethylene-*alt*-maleic anhydride) (B). Computer graphics and conformational analysis were applied to construct models of the pure components A and B. Possible hydrogen bonding interactions in the A/B blend were then proposed based on visual inspection of the alignment of functional groups. Quantum mechanical calculations were applied to these models to search for the existence of attractive interactions between the chains. The hydrogen bonding was postulated to involve mainly the oxygen atoms of poly(ethylene-*alt*-maleic anhydride) (PEMA) and the tertiary hydrogens of polyacrylonitrile (PAN). The possibility of weak interactions between the nitrogen atoms of PAN and the tertiary hydrogens of PEMA was also visualized. All favorable conformations indicated a high probability for a dense packing of the two dissimilar polymer chains. The electron density diagrams characteristics to these conformations also suggested interactions, although weak.

INTRODUCTION

In recent years, one of the main features of polymer science has been the exploitation of polymer–polymer blending to provide new high performance materials [1–3]. The success of this approach is best illustrated by the fact that a large number of polymer blends were introduced to fulfill specific needs or to add valuable properties to the existing materials. In a closely connected way, strong impetus for elucidating polymer–polymer miscibility/immiscibility behavior in order to provide further insight into polymer blending approach has evolved. Many studies are devoted to the concept of mixing polymeric chains containing different functional groups capable of interactions. Enhanced or complete miscibility due to specific interactions such as hydrogen bonding formation between proton-donating and proton-accepting groups of the two components of the blend were reported [1–6]. Other types of interactions include electron donor–electron acceptor (EDA) bonds arising from situations where the molecules of one component are electron donors while of the other are electron acceptors [7, 8].

The complexity of polymer–polymer interactions and the difficulties encountered in the characterization and correct interpretation of the phase behavior of polymer blends requires the rapid survey of the effect of changing one or more variables. Chain conformations and interactions at the molecular and segmental level in polymer blends can be approximately taken into consideration using a computer modeling approach.

In this contribution an example of the power of molecular modeling will be illustrated as applied to understanding the molecular architecture of a binary miscible polymer blend. The structural units of the two partners of the blend system under investigation are derived from acrylonitrile and ethylene–maleic anhydride alternating copolymers, respectively. Because of the large number of structural features that are present in this system, the study is not meant to recommend a specific modeling path or to suggest that the proposed models are supplying a definite answer. The conformations assumed are, if anything, a convenient starting point. This exercise can be further expanded, and the models can be refined, which ultimately may lead to correlations between the molecular level properties and macroscopic behavior of polymer–polymer homogeneous mixed phases.

Binary blends of high nitrile polymers such as acrylonitrile/methyl acrylate/butadiene terpolymer (AN/MA/BU = 70/21/9) (Barex 210) and poly(ethylene-*alt*-maleic anhydride) (PEMA) have been reported to be miscible based on optical transparency and DSC data [9]. The glass transition-temperatures of this blend system vary monotonically with composition, following equations such as Gordon–Taylor [10] and Kwei [11]. The monophase behavior of these blends was also clearly demonstrated by solid-state cross-polarization (CP-MAS) NMR [12]. These systems exhibit single component rotating frame spin-lattice relaxation times intermediate in value as compared to the pure components. The formation of such a homogeneous monophase blend is attributed to a favorable heat of mixing arising from some specific interactions between the two component polymers. An FT-IR study conducted on Barex 210/PEMA blends [13] evidenced a shift in the nitrile absorption peak of Barex 210 and in carbonyl absorption peak of PEMA. This clearly indicates the involvement of these groups in nonbonding interactions. Interestingly, these blends also show a high ability to restrict the passage of gas molecules

such as O_2 and CO_2. The gas barrier properties of B210/PEMA blends are in fact significantly better than those of Barex 210 component which is already known as a high barrier polymer. This behavior can be related to the conformational changes/arrangements of the two polymeric chains during blending. The decrease in gas permeability may indicate an increased stiffness or a decrease in the mobility of the polymer chain segments due to the interaction of the two polymers. Based on these assumptions, a close chain packing can also be suggested. The latter is supported by experimental evidence. For example, the densities of the miscible blends are higher than the calculated values based on volume additivity of the two components.

Questions regarding the relationship existing between the molecular architecture of this blend and its unique gas barrier properties are not only intriguing, but valuable for practical reasons. Thus, we searched for answers with the power of computer modeling technique. To eliminate complicating effects arising from interactions of different types of groups in a polymer blend, polyacrylonitrile (PAN) was substituted for Barex 210 in our model. The blend system under investigation was limited to the following two repeat units:

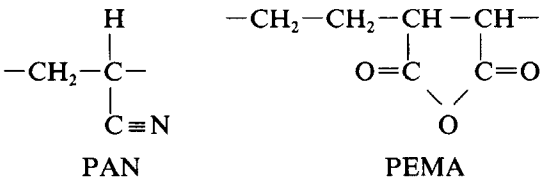

Since experimental evidence, previously mentioned, has suggested interactions involving the nitrile groups of Barex and carbonyl groups of PEMA, our simplified PAN-PEMA model would seem to retain the most important features of the Barex-PEMA system.

RESULTS AND DISCUSSION

Construction of the Model

Almost all useful properties of polymers can be described in some way by the conformational characteristics of the component molecules. Generally, the molecules will alter their geometry by torsional rotations or "twisting motions" of their covalent bonds in order to achieve the conformation which gives the lowest free energy to the system. The conformational search on the architecture of the two polymers involved in this study followed the sequences of operations shown below.

Conformations of PEMA Segments

Two models of short segments of PEMA were constructed. Bond length and bond angle values were held constant at conventional values, while torsional angles along the chain were systematically varied. For each conformation, the energy was calculated by a simple empirical force field expression. From these considerations, two plausible (not necessarily optimum) conformations for the PEMA chain were chosen. They are shown in Figs. 1(a) and 1(b). For comparison, the low energy conformations from the conformational analyses are also shown, in Figs. 2 and 3.

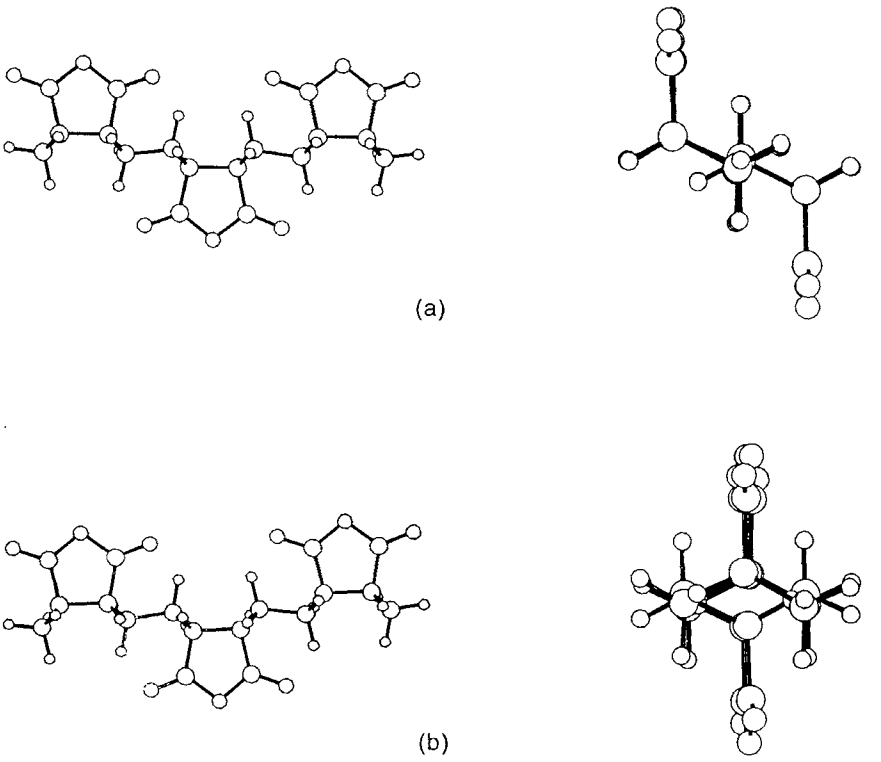

FIG. 1. Two proposed structures for PEMA. In Structure 1(a) the chain continues from the same side of the ring. In Structure 1(b) the chain continues from the opposite side of the ring.

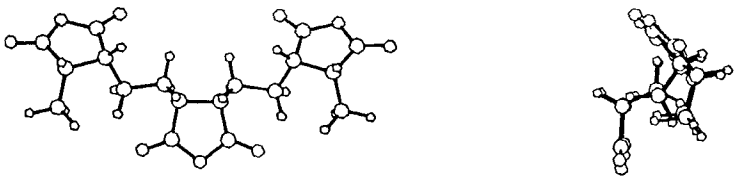

FIG. 2. Result of conformational analysis applied to Structure 1(a) of PEMA.

Conformations of PAN Segments

Three structures for the PAN chain were considered. These are shown in Figs. 4(a), 4(b), and 4(c).

Selection of PAN–PEMA Orientation

Orientations of PAN relative to PEMA were explored by computer graphics. Of particular interest were orientations which might involve interchain interactions with the nitrile or carbonyl groups. One such arrangement is shown in Fig. 5.

Optimization of the PAN–PEMA Interactions

Quantum mechanical calculations with Austin Model 1 (AM1) method [14, 15] were applied to three particular arrangements of PAN interacting with PEMA. In each of the three classes an optimization of the interaction between rigid fragments of PAN and PEMA was carried out. The starting points for these optimizations are shown in Figs. 6(a), 7(a), and 8(a).

Electron Density for Interchain Interactions

Electron density between a pair of atoms is one way to evaluate the extent of interaction between atoms. From the wave functions of the calculations above, electron density contours were displaced. These are shown in Figs. 9, 10, and 11.

Computational Procedures

For the general approach described above, the specific computational procedures are described below.

Conformations of PEMA Segments

Conformational analysis was applied to the PEMA structures shown in Figs. 1(a) and 1(b). Four rotatable bonds of the backbone were selected in each case. For

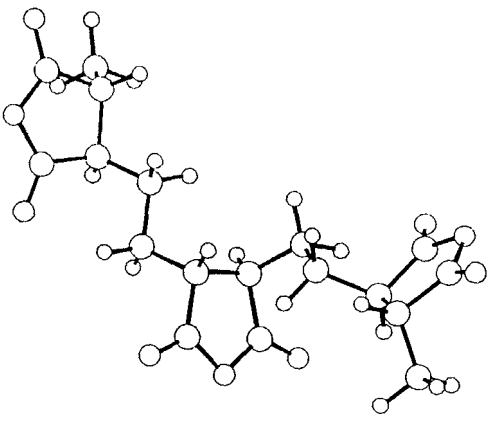

FIG. 3. Result of conformational analysis applied to Structure 1(b) of PEMA.

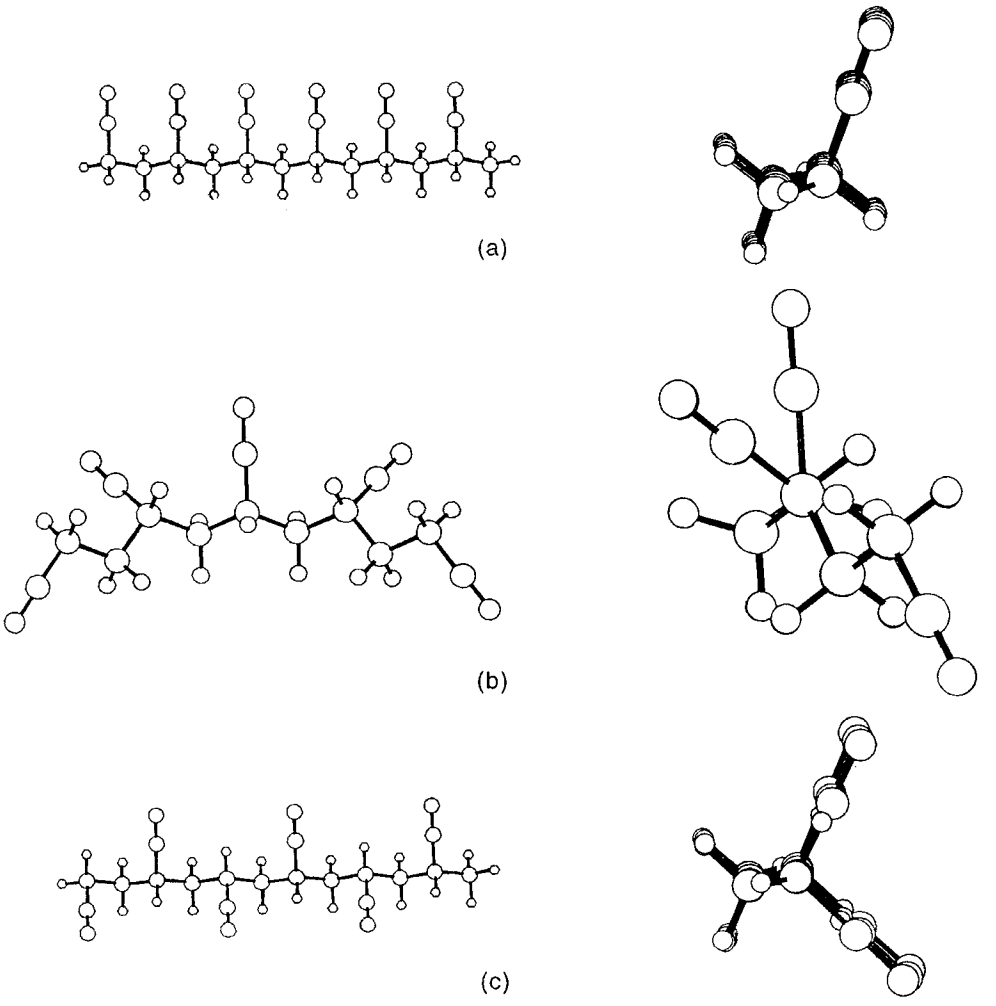

FIG. 4. Three proposed structures for PAN. The syndiotactic conformation shown in Fig. 4(a) is the actual structure used in the calculations reported in this paper. Structure 4(b) is just another lower energy conformation of syndiotactic Structure 4(a). Structure 4(c) is the conventional isotactic configuration of PAN.

the structure of Fig. 1(a), each bond was rotated through 360° by 30° increments. For the structure of Fig. 1(b), 60° increments were used. The energy was calculated at each conformation using a functional form and parameterization of Del Re and Giglio [16] as implemented within Chemx [17]. This includes the following terms:

$$V_{\text{pot}} = \frac{A \exp(-Br)}{r^D} - \frac{C}{r^6} \tag{1}$$

where r is the internuclear separation distance between two atoms in Å, and A, B, C and D are constants.

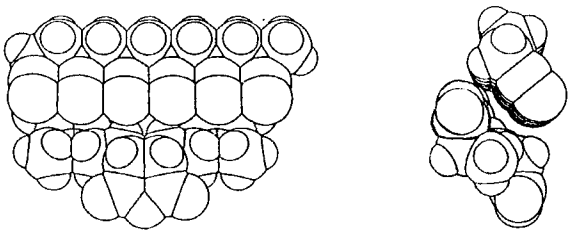

FIG. 5. A possible PAN/PEMA orientation identified by visual screening.

•The electrostatic energy function (extended to a simple electrostatic V_{el})

$$V_{el} = \frac{KQ_1Q_2}{er} \tag{2}$$

where Q_1 and Q_2 are the electronic charges of the two atoms (in unitless partial charges)
e is the dielectric constant
K is a conversion constant.

•The torsional term (V_t)

$$V_t = T[(1 + \cos(3W)] \text{ about nonconjugated bonds} \tag{3}$$

where T is a user-defined constant for each pair of atom types.

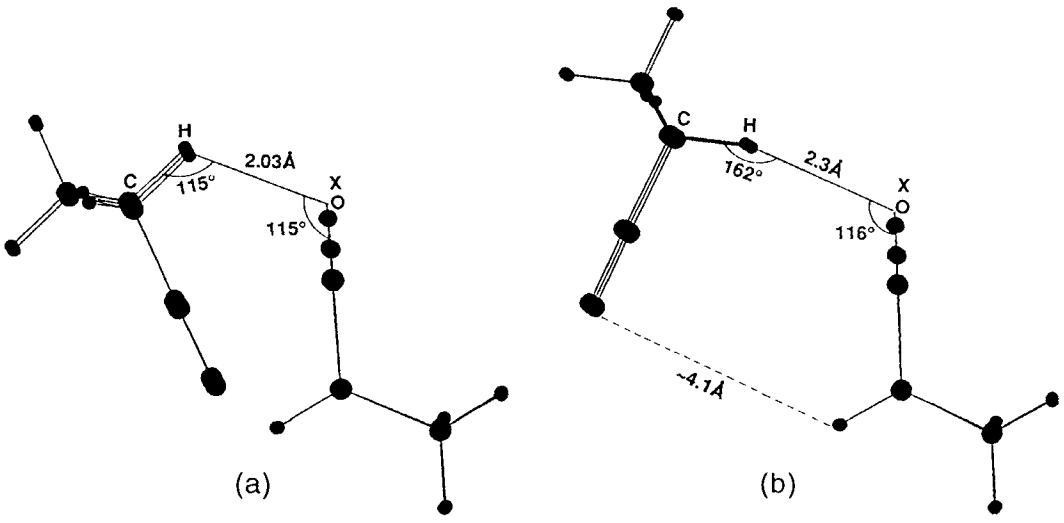

FIG. 6. Structures 6(a) and 6(b) show the starting point for a geometry optimization and the optimization using AM1, applied to PAN shown in Fig. 4(a) and PEMA in Fig. 1(a), respectively.

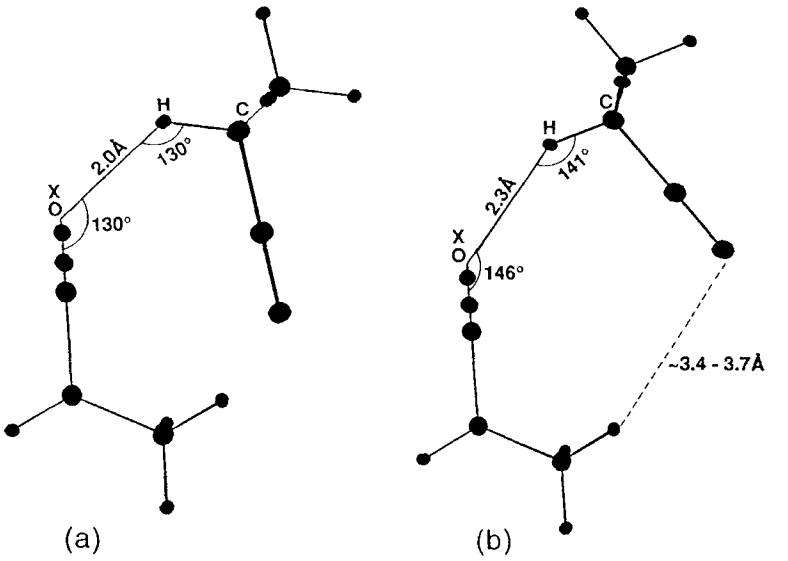

FIG. 7. The same structures as the structures from Figs. 6(a) and 6(b) except the PAN is on opposite side of the ring of the PEMA chain.

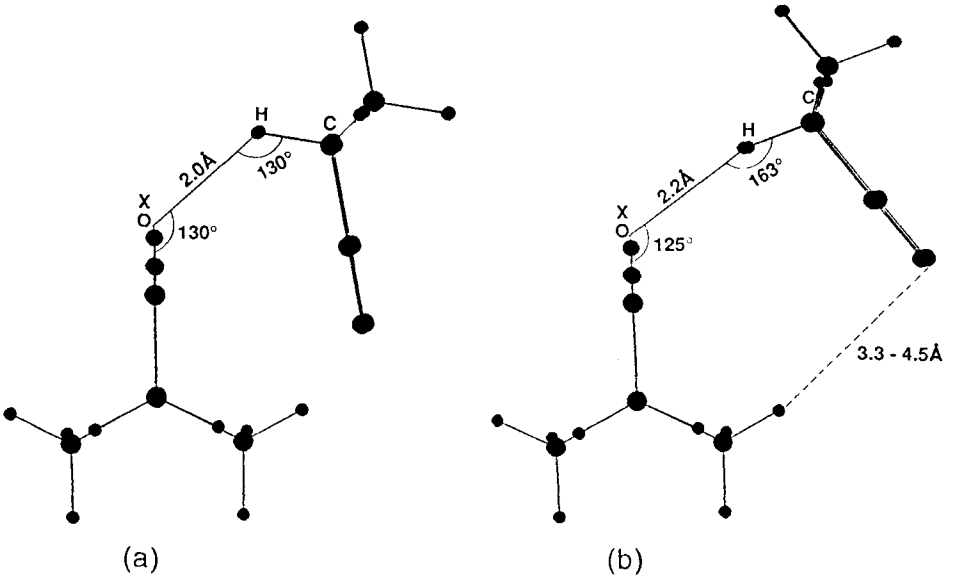

FIG. 8. The same structures as the structures from Figs. 6(a) and 6(b), except using PEMA as in Fig. 1(b).

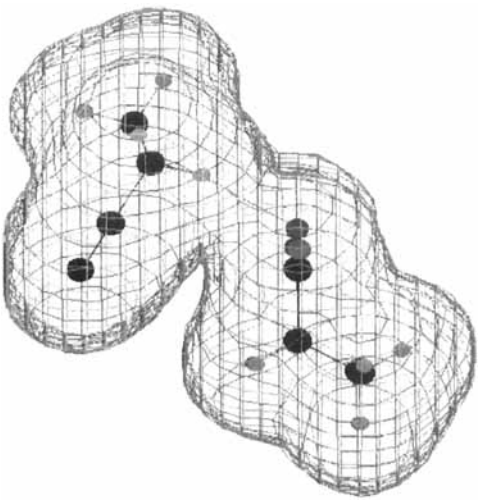

FIG. 9. Electron density map showing weak interactions between chains of PAN and PEMA for the optimized structure of Fig. 6(b).

•The total nonbonding interaction energy, E_{vdw}, is the sum of all the interactions between all nonbonded atom pairs:

$$E_{vdw} = (V_{pot} + V_{el} + V_t) \tag{4}$$

Thus, for the structure of Fig. 1(a) Eq. (1) to (4) were applied to $12^4 = 20{,}736$ conformations, and for the structure of Fig. 1(b), $6^4 = 1296$ conforma-

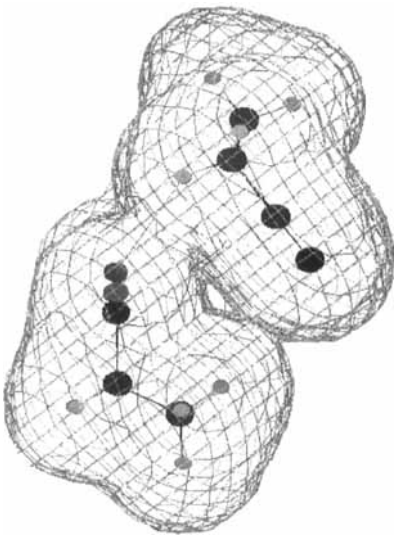

FIG. 10. Electron density map for the optimized structure of Fig. 7(b).

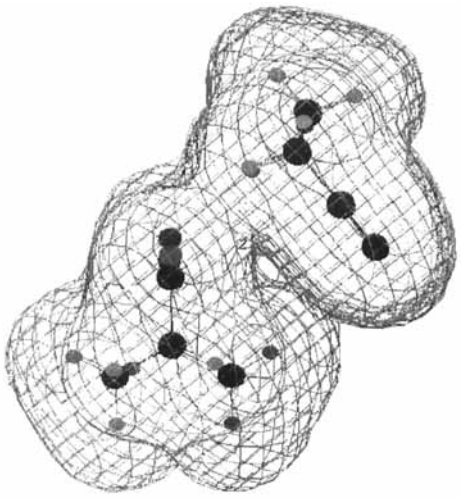

FIG. 11. Electron density map for the optimized structure of Fig. 8(b).

tions. The lowest energy conformations found by each of these conformational analyses are shown in Figs. 2 and 3. Figure 2 corresponds to the structure of Fig. 1(a), while Fig. 3 corresponds to the structure of Fig. 1(b).

Based on these limited calculations and examining other low-energy conformations in addition to those shown in Figs. 2 and 3, the backbone of an isolated chain of PEMA is likely to be arranged such that consecutive rings are relatively far apart. This, of course, is entirely consistent with intuition. For convenience and to have a simple but definite conformation for each of the two chains, the structures shown in Figs. 1(a) and 1(b) were selected. Both structures are highly symmetrical, with the backbone geometry repeating after just two chemical repeat units. The conformational energy of the structure of Fig. 1(a) is 21.4 kcal/mol above the low energy conformation of Fig. 2. The structure of Fig. 1(b) is 8.1 kcal/mol above the conformation of Fig. 3.

Conformation of PAN Segments

Figure 4 shows the three PAN structures considered. Conformational analysis using the same functions as described above (Eqs. 1 to 4) was also carried out for a 5-repeat units PAN chain. Eight bonds along the main chain were allowed to rotate by 60° through 360°. To calculate every point of such a conformational search, Eq. (4) would need to be evaluated for each of $6^8 = 1{,}679{,}616$ conformations. In order to make the conformation of more manageable size, several conformations were rejected based on geometrical considerations before calculating the energy [Ref. 17, Section 4.4.2]. The minimum energy conformation found by this calculation is the structure shown in Fig. 4(b).

The structure of Fig. 4(a) is a rather high-energy conformation for PAN. The comparable 5-repeat units PAN chain which is the starting point for the conformational analysis of the previous paragraph is above the minimum energy conformation. For calculations described below, however, we did use this high energy confor-

mation because it presents interesting possibilities for the interaction with a PEMA chain. For comparison, the more conventional isotactic PAN structure is shown in Fig. 4(c).

Selection of PAN–PEMA Orientation

We used interactive computer graphics to manipulate PEMA and PAN fragments to find orientations of one fragment relative to the other which present possibilities for attractive interchain interactions. Figure 5 shows one arrangement which was identified by this procedure. Two other PAN–PEMA arrangements were also identified. These orientations were then used as starting points for geometry optimizations by the quantum mechanics AM1 method. However, even with the small PEMA fragments shown in Fig. 1, and the PAN fragments of Fig. 4, the resulting PAN–PEMA structure is larger than we could conveniently handle with an AM1 calculation (the limit is with our computational environment rather than a fundamental limit on AM1). Thus we restricted PEMA to one chemical repeat unit, and PAN was restricted to three units. Each of these two fragments was considered rigid, but they were allowed limited motion relative to each other.

Optimization of the PAN–PEMA Interactions

To help define the initial geometries and the optimization variables, a fictitious atom X connected to both PEMA and PAN was defined. Figure 6(a) illustrates one initial geometry and the one distance and two angles which are the degrees of freedom for an optimization. The variables to be optimized are the following: (a) the movement of the PAN chain closer to or further from the PEMA fragment; (b) the rotation of PAN about PEMA while keeping the PAN and PEMA chains parallel; and (c) the rotation of PAN about an axis parallel to its backbone. This should allow at least partial optimization of any "bonding" distances and angles between the PAN and PEMA chain.

Figure 6(a) shows the initial geometry for one particular optimization. This case uses a shortened form of the PEMA structure of Fig. 1(a). Figure 7(a) shows another starting point, using the same PEMA structure as in Fig. 1(a), but with PAN on the opposite side of the PEMA ring compared to its location in Fig. 6(a). A third starting geometry is shown in Fig. 8(a) using a fragment of the PEMA chain of Fig. 1(b). For each of these three optimizations, two angles (C—H—X and H—X—O) and one distance (HXX) are allowed to change, allowing rigid PAN to move with respect to rigid PEMA as described in the previous paragraph.

The optimization was carried out by using the method AM1 in the quantum chemistry program AMPACX [Ref. 15 and QCPE 506]. Figures 6(b), 7(b), and 8(b) show optimized values of the variables which were allowed to change. These variables all involve the arbitrarily-placed fictitious atom X, and therefore, their values are not of fundamental chemical significance. A more meaningful measure is the angle between the —C—H bond of PAN and the planar (or nearly planar) ring of PEMA. This was calculated by letting three atoms of the ring (the oxygen atom, and the two carbon atoms which are part of the PEMA backbone) define a plane, and then calculating the angle between the plane and the bond C—H bond "connected" to atom X in Figs. 6 to 8. In each case, this angle is very close to the tetrahedral angle.

Two additional distances for the optimized structures are shown in Figs. 6(b), 7(b), and 8(b). One is the distance between atom H of PAN and atom O1 of PEMA (Fig. 6b); the other one represents the range of distances between the N atoms of PAN and the H atoms of the PEMA chain (Figs. 7b and 8b).

Electron Density Diagrams for Interchain Bonds

Electron density diagrams were calculated by the program DENPOT, as implemented in Chemx [DENPOT, QCPE 483]. The results, presented as wire frames representing dimensional contours with a density of 0.005 (a low value compared to typical densities between bonds), are shown in Figs. 9, 10, and 11.

CONCLUSIONS

Molecular modeling was applied to describe the molecular architecture in a homogeneous A/B (PAN/PEMA) blend system. Models of the pure components A and B and of their blends have been constructed based on both conformational analysis and computer graphics. Favorable conformations may indicate the probability of intermolecular interactions suggested by experimental IR and NMR data. These interactions that appear to involve nonbonding attractions are favorable for the generation of close-packing arrangement between neighboring dissimilar chains. The electron density maps also suggest the probability of the arrangement of the two polymer chains in a closely-packed manner. Evidently, a more rigorous modeling treatment of this system is required since both components possess multiatomic side groups which can undergo complex torsional motions. New minima (or global minimum) which may be present in conformational space not searched in our study, as well as the effect of intramolecular bonding or conformation and the extent of intersegment bonding, should be considered.

ACKNOWLEDGMENT

The authors wish to express their thanks to Dr. John Kerins for many helpful discussions and suggestions.

REFERENCES

[1] M. M. Coleman, J. F. Graz, and P. C. Painter, *Specific Interactions and the Miscibility of Polymer Blends*, Technomic Publishing Co., Lancaster, Pennsylvania, 1991.

[2] L. A. Utracki, *Polymer Alloys and Blends. Thermodynamics and Rheology*, Hanser Publishing Co., New York, 1989.

[3] S. Lu, E. M. Pearce, and T. K. Kwei, *J. Macromol. Sci.—Pure Appl. Chem., A31*, 1535 (1994).

[4] M. Aubin and R. E. Prud'homme, *Macromolecules, 13*, 365 (1980).

[5] T. K. Kwei, E. M. Pearce, J. R. Pennachia, and M. Chartoon, *Ibid., 20*, 1174 (1987).

[6] G. Guerra, D. J. Williams, F. E. Karasz, and W. J. MacKnight, *J. Polym. Sci., Polym. Phys. Ed., 26*, 301 (1988).
[7] J. M. Rodriquez-Parada and V. Percec, *Macromolecules, 19*, 55 (1986).
[8] C. Pugh and V. Percec, *Ibid., 19*, 65 (1986).
[9] S. Percec and L. Melamud, *High Performance Polym., 1*, 73 (1989).
[10] M. Gordon and J. S. Taylor, *J. Appl. Chem., 2*, 485 (1952).
[11] T. K. Kwei, *J. Polym. Sci., Polym. Lett. Ed., 22*, 307 (1984).
[12] S. Percec and T. Hammond, *Polymer, 32*, 1252 (1991).
[13] S. Percec and R. Barbour, Unpublished Results.
[14] T. A. Clark, *Handbook of Computational Chemistry. A Practical Guide to Chemical Structure and Energy Calculations*, Wiley, New York, 1985.
[15] M. J. S. Dewar, E. G. Zoebisch, E. F. Healy, and J. J. P. Stewart, *J. Am. Chem. Soc., 107*, 3902 (1985).
[16] G. Del Re and E. Giglio, *Acta Crystallogr., 1333*, 3289 (1977).
[17] Chemical Design Ltd., *The Chemx Suite Reference Manual*, Oxford University Press, Oxford, 1988.